Supporting Information

Heuberger et al. 10.1073/pnas.1309342111

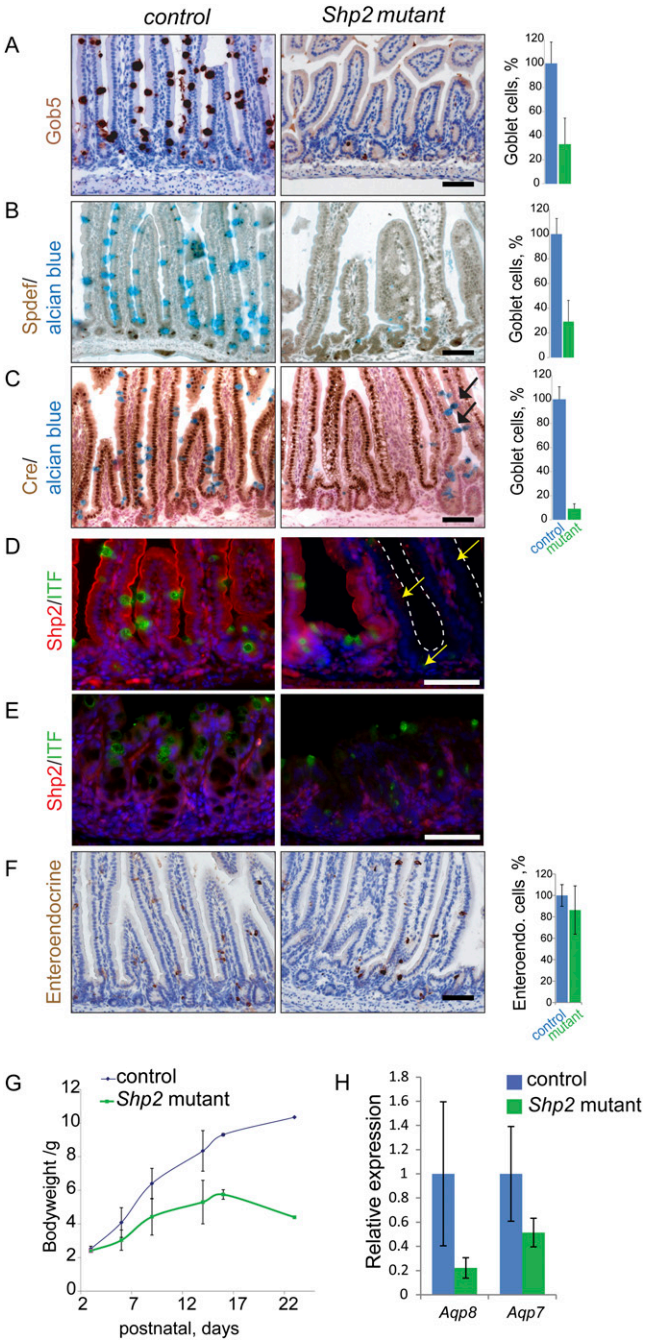

Fig. S1. (*A* and *B*) Staining of goblet cells for chloride channel calcium activated 3 (Clca3, also known as Gob5) and SAM pointed domain containing ets transcription factor (Spdef)/alcian blue on sections of control and *Shp2* mutant intestines at P9; quantification of goblet cells is on the right ($n = 4$). (*C*) Staining for Cre-recombinase (brown, nuclear) and goblet cells (alcian blue) on sections of control and *Shp2* mutant intestines at P9, which show few remaining goblet cells in areas with low Cre expression (see arrows on the *Right*); overall quantification of goblet cells in the majority of high Cre-expressing villi is on the *Right* ($n = 4$). (*D* and *E*) Staining for Shp2 (red) and intestinal trefoild factor (ITF)-positive goblet cells (green) on sections of control and *Shp2* mutant small intestines (*D*) and colons (*E*). (*F*) Staining of enteroendocrine cells for ChromagraninA on sections of control and *Shp2* mutant intestines at P9; quantification is on the *Right* ($n = 4$). (*G*) Growth retardation of conditional *Shp2* mutants after birth, compared with controls. (*H*) Decreased mRNA expression of *Aqp8* and *Aqp7* in *Shp2* mutants, assessed by qRT-PCR ($n = 5$). (Scale bars, 100 μm.)

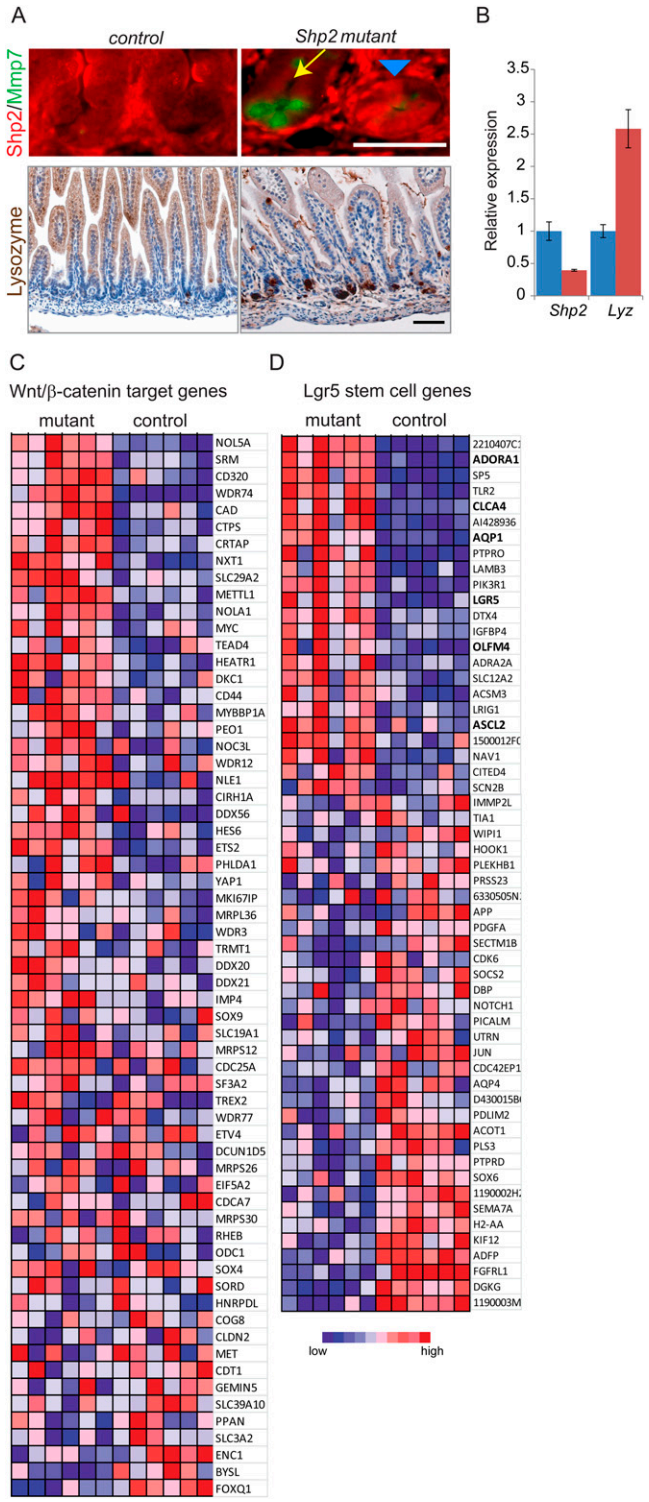

Fig. S2. (*A*) Immunofluorescence of Shp2 and Mmp7-positive paneth cells (*Upper*, yellow arrow points to Shp2-deficient crypt with paneth cells, blue arrowhead points to nonrecombined crypt without paneth cells) and immunhistology of lysozyme-positive paneth cells (*Lower*). (*B*) Expression of *Shp2* and *Lysozyme* mRNAs in control (blue bars) and *Shp2* mutant organoids (red bars) after tamoxifen-induced mutagenesis, assessed by qRT-PCR. (*C* and *D*) Gene set enrichment analysis (GSEA) heatmaps of control versus *Shp2* mutants for Wnt/β-catenin target genes and for down-regulated genes of the Lgr5+ stem cell signature.

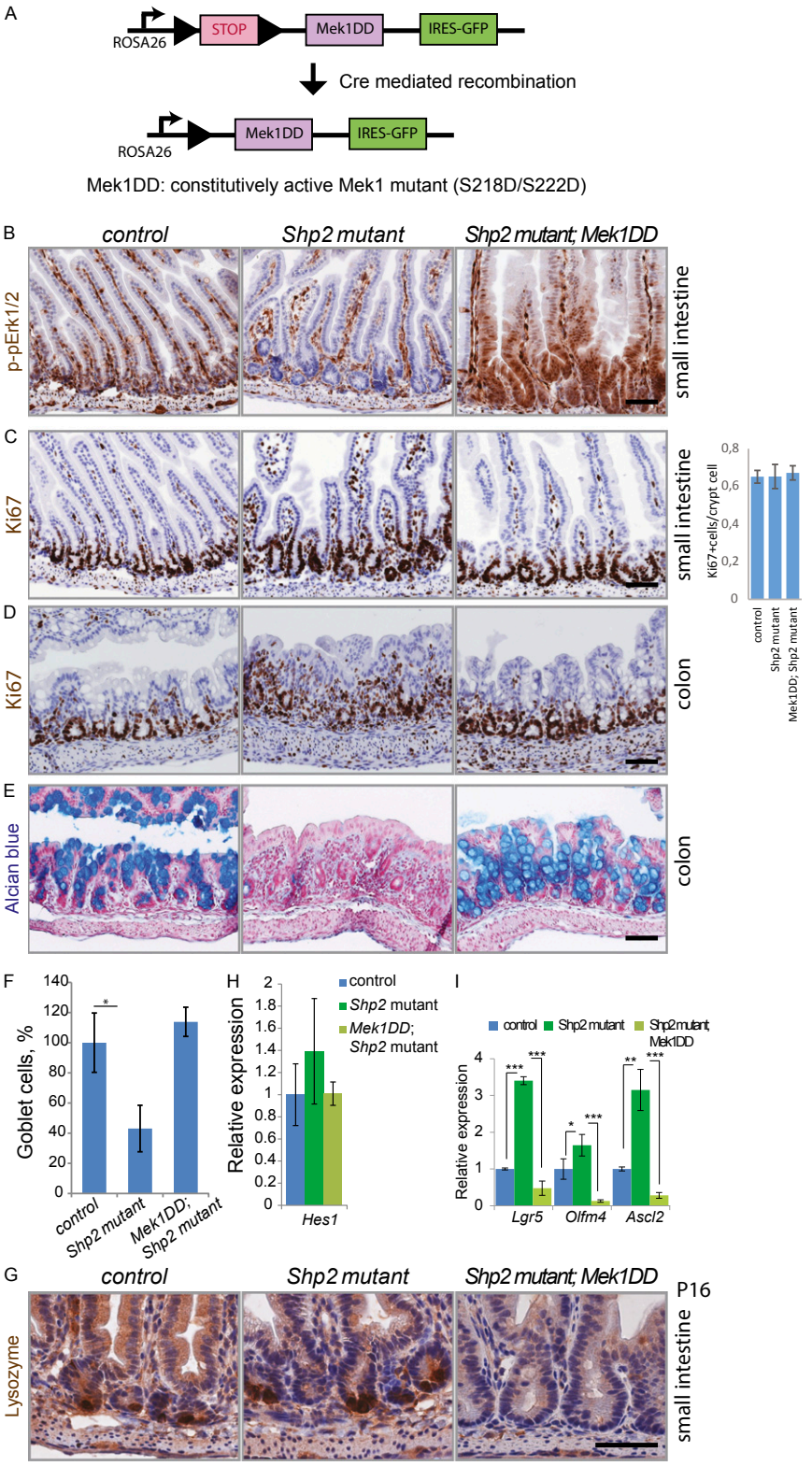

Fig. S3. (*A*) Scheme of the *Mek1DD* allele. The *ROSA26* allele harbors the cDNA of a gain-of-function variant of Mek1, preceded by a *loxP*-flanked STOP cassette and followed by an *eGFP* gene under the control of an internal ribosomal entry site (1). *Mek1DD* is expressed upon removal of a translation stop cassette through Cre-mediated recombination. (*B*) Altered MAPK signaling in the small intestine of *Shp2* mutant and compound *Shp2; Mek1DD* mutant mice at P6, assessed by immunohistochemistry for pErk. (*C* and *D*) Immunohistology for proliferating cells with anti-Ki67 antibody of P6 sections of small intestines and colon (marked on the *Right*), *Shp2* and compound *Shp2; Mek1DD* mice (quantification is on the *Right*). (*E*) Rescue of the goblet cell phenotype in the *Shp2* mutant colon by *Mek1DD*; goblet cells stained with alcian blue. (*F*) Quantification of goblet cells in *Shp2* mutant and compound *Shp2; Mek1DD* mutant small intestines at P6 ($n = 3$). (*G*) Immunohistology of paneth cells of small intestines at P16 stained for lysozyme. (*H*) *Hes1* expression in P6 control, *Shp2*, and

Legend continued on following page

compound *Shp2; Mek1DD* mice determined by qRT-PCR ($n = 3$). (*I*) Rescue of *Lgr5*, *Olfm4*, and *Ascl2* mRNA expression in *Shp2* mutants by *MekDD1,* assessed by qRT-PCR. Significance calculated with *t* test; $*P < 0.05$, $**P < 0.01$, $***P < 0.001$. (Scale bars, 100 μm.)

1. Srinivasan L, et al. (2009) PI3 kinase signals BCR-dependent mature B cell survival. *Cell* 139(3):573–586.

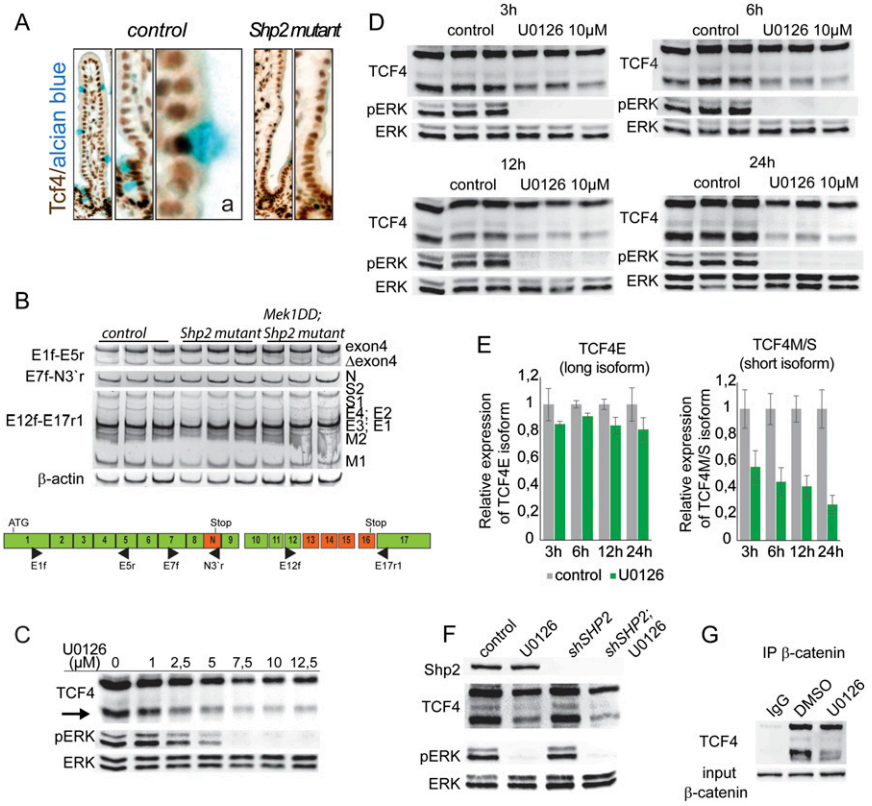

Fig. S4. (*A*) Staining for Tcf4 and goblet cells (alcian blue) of control and *Shp2* mutant small intestines. An enlargement (a) of control is also shown. (*B, Upper*) Analysis of *Tcf4* splice variants on the mRNA level of intestinal organoids of tamoxifen-inducible *Shp2* mutants, *Mek1DD; Shp2* double mutants and controls. (*Lower*) Scheme of exons of *Tcf4* cDNAs with primer binding sites and the classifications of splice variants is based on Weise et al. (1). (*C*) Dependence of TCF4 isoform changes on the concentration of the MEK1/2 inhibtior UO126 in HT29 cells. (*D*) Reduction of the short TCF4 splice variants after 3, 6, 12, and 24 h of MEK1/2 inhibition in HT29 cells. Triplicate cell cultures were examined. (*E*) Quantification of changes of the TCF4 isoforms upon MEK1/2 inhibition by measuring the signal intensities from *D*; no significant changes of the long TCF4 isoform (diagram on the *Left*) and decrease of the short TCF4 isoform (diagram on the *Right*) upon MEK1/2 inhibition (green bars) ($n = 3$). (*F*) Knockdown of *SHP2* by shRNAs in HT29 has no effect on ERK activity and TCF4 isoform production. (*G*) Coimmunoprecipitations of TCF4 with β-catenin from nuclear fractions; interaction of β-catenin with TCF4E persists after 6 h of MEK1/2 inhibition.

1. Weise A, et al. (2010) Alternative splicing of Tcf7l2 transcripts generates protein variants with differential promoter-binding and transcriptional activation properties at Wnt/beta-catenin targets. *Nucleic Acids Res* 38(6):1964–1981.

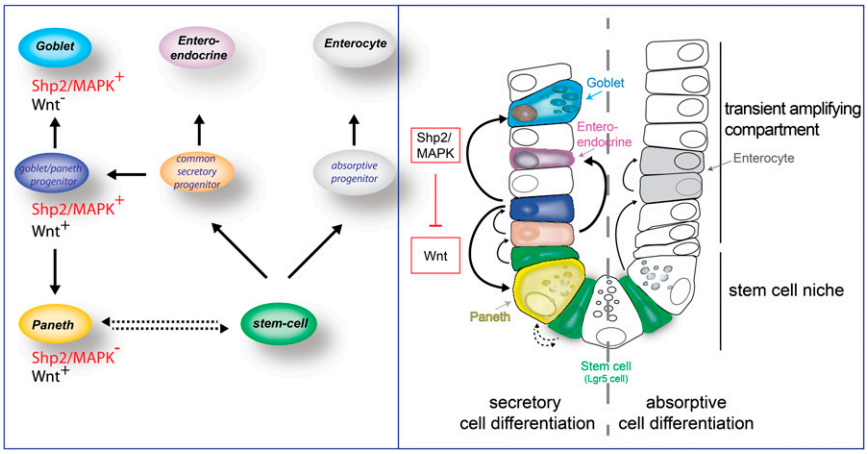

Fig. S5. Schemes of intestinal cell differentiation. (*Left*) Cell types and intrinsic signaling. Shp2/MAPK activity (red) regulates the differentiation of goblet cells, which are MAPK+ Wnt−, and paneth cells, which are MAPK− Wnt+ after progenitor specification into a common goblet/paneth cell progenitor. Enteroendocrine cells separate earlier, i.e., from a general secretory progenitor in a Shp2/MAPK-independent manner. Shp2/MAPK exerts this function by blocking Wnt/β-catenin signaling. (*Right*) Cell differentiation in the stem cell niches and in the transient amplifying compartments. The inhibitory effect of Shp2/MAPK on Wnt signaling is shown in red. The common secretory progenitor is marked as +5.